Narrative Review Article

Nanotheranostics for Cancer: Integrating Imaging, Therapy, and Real-Time Monitoring

Trisha Manipatruni

Dougherty Valley High School, 10550 Albion Rd, San Ramon, CA 94582, United States

ABSTRACT

Despite decades of progress, cancer is still frequently detected only at advanced stages, and conventional treatments such as surgery, chemotherapy, and radiation therapy often lack tissue specificity. These limitations have motivated the development of approaches that unify early detection with targeted treatment in a single system. A nanotheranostic platform is an engineered nanoparticle construct that integrates therapeutic and diagnostic functions within a single system. In preclinical studies conducted both *in vitro* and in animal models, such platforms have shown early evidence of the capacity to improve lesion visualization, enable image-guided treatment activation, and support treatment-response monitoring. This review breaks down nanotheranostic platforms into three core design dimensions: therapeutic modality (including photothermal therapy (PTT), photodynamic therapy (PDT), chemotherapy, and multimodal systems), diagnostic readout (primarily fluorescence and magnetic resonance imaging (MRI)) and targeting strategy (including passive accumulation via the enhanced permeability and retention (EPR) effect, ligand-mediated active targeting, and organelle localization). By integrating diagnostic and therapeutic components, these platforms are designed to increase tumor-associated delivery and enable image-guided activation, with reported improvements in tumor control in preclinical models. Across cited studies, multimodal nanotheranostic systems often demonstrate improved tumor control relative to single-modality comparators within the same experimental model. However, reductions in systemic toxicity and improvements in patient quality of life remain unverified in clinical settings. To identify the most promising clinically translatable strategies, this review examines critical barriers to translation, including immune clearance, batch-to-batch variability, manufacturing scale-up, regulatory complexity, and long-term biodistribution. The review concludes by identifying design principles associated with stronger translational positioning compared to platforms that remain preclinical.

Keywords: cancer; nanotheranostics; theranostics; nanomaterials; nanoscience

INTRODUCTION

Cancer continues to be a leading cause of death worldwide. In 2022, there were about 20 million new cases and nearly 10 million deaths globally (1). By 2050, annual cases are projected to reach about 33 million, and the number of cancer-related deaths will rise to 18.2 million (1). These trends reinforce the demand

Corresponding author: Trisha Manipatruni, E-mail: trisha.manipatruni@gmail.com.

Accepted March 11, 2026
https://doi.org/10.70251/HYJR2348.42126136

for earlier detection and more tumor-specific treatment strategies (2).

Current diagnostic tools have major drawbacks. Limited sensitivity and specificity can delay detection, thereby reducing treatment options and worsening outcomes (2, 3). Conventional imaging modalities such as computed tomography (CT) and magnetic resonance imaging (MRI) are essential for staging and treatment planning, yet sensitivity can be limited for very small lesions and microscopic disease. Confirmation of cancer still requires an invasive biopsy that samples only a small portion of the suspect tissue (3, 5). On the therapeutic side, chemotherapy and radiation therapy lack specificity and thus damage healthy tissues, causing severe side effects that limit the doses patients can tolerate (2, 3). Achieving tumor-targeted delivery is still a major challenge (3, 6). Although recent modalities such as immune checkpoint inhibitors, chimeric antigen receptor T-cell (CAR-T) therapy, gene-based approaches, and targeted agents such as poly(ADP-ribose) polymerase (PARP) inhibitors have improved outcomes in certain cancers, a substantial proportion of patients either fail to respond, develop resistance, or experience considerable toxicity. Furthermore, delivery barriers and tumor heterogeneity continue to restrict the precision and efficacy of these therapies.

These diagnostic and therapeutic limitations have increased interest in nanotheranostic systems that integrate sensitive imaging, targeted delivery, and treatment monitoring into a single platform. In this work, a nanotheranostic platform is defined as a nanoscale construct that integrates a therapeutic function with a diagnostic readout in a functionally linked manner (2, 3, 7). Specifically, the same nanoparticle must (i) deliver or activate a therapeutic intervention and (ii) generate a measurable signal that reports on localization, drug release, target engagement, or treatment response and use that diagnostic information to guide or evaluate its own therapeutic action.

This review organizes nanotheranostic platforms into three domains. The first covers therapy modalities, including photothermal therapy (PTT), in which light-absorbing agents convert near-infrared (NIR) irradiation into localized heat; photodynamic therapy (PDT), where a photosensitizer generates cytotoxic reactive oxygen species (ROS) upon light activation; conventional chemotherapy, which relies on cytotoxic drugs that disrupt cell proliferation; and combination platforms that integrate two or more of these treatments within a single construct. The second covers diagnostic readouts, including MRI, which provides deep-tissue anatomical and functional contrast, often enhanced by contrast agents, and fluorescence imaging, which uses emissive probes to visualize nanoparticle localization and, in some cases, report microenvironmental cues. The third covers targeting strategies, including passive targeting via the enhanced permeability and retention (EPR) effect, where nanoparticles accumulate due to leaky tumor vasculature and poor lymphatic drainage; ligand-based active targeting, in which antibodies, peptides, aptamers, or small molecules bind overexpressed receptors to promote cellular uptake; and organelle targeting, where localization motifs direct payloads to compartments such as mitochondria, lysosomes, or nuclei to increase on-target damage. Building on this framework, the review examines design trade-offs for integrated systems that combine chemotherapy, phototherapy, and imaging within a single platform.

It is important to note that the majority of nanotheranostic findings discussed in this review derive from *in vitro* cell studies and *in vivo* animal models. These promising results in *in vitro* and *in vivo* models highlight the potential of nanotheranostic platforms for cancer treatment and support further investigation toward clinical development. Despite their promise, nanotheranostic platforms face several well-recognized barriers to clinical translation that are critically examined throughout this review. These include rapid immune clearance by the mononuclear phagocyte system, which can reduce circulation time and limit tumor accumulation (2, 11); batch-to-batch variability in nanoparticle synthesis, which complicates reproducibility and quality control (6); challenges in manufacturing scale-up from laboratory to clinical grade production; regulatory complexity surrounding the approval of combination drug-device constructs; and concerns about long-term biodistribution and clearance of nanoparticle components (2, 6, 12). These challenges represent critical gaps between preclinical promise and demonstrated clinical utility.

THERAPEUTICS

Four therapeutic modalities are examined in this review: PTT, PDT, chemotherapy, and combination platforms. Each modality is described in terms of its core mechanisms and illustrated by a representative benchmark nanoplatform, as summarized in Figure 1 and Table 1.

Table 1. *This table summarizes representative preclinical nanoplatforms (material class and formulation features) and links each to its therapy modality (e.g., chemotherapy, photothermal therapy [PTT], photodynamic therapy [PDT], radiotherapy enhancement, immunomodulation), imaging modality (e.g., fluorescence [FL], photoacoustic [PA], MRI, CT, PET), and targeting strategy (passive/enhanced permeability and retention [EPR] vs. active ligand–receptor targeting). Abbreviations: IV, intravenous; SubQ, subcutaneous mouse flank xenograft; U87MG, human glioblastoma xenograft; Raji, human B-cell lymphoma xenograft; KB, human oral epidermoid carcinoma cell line; MDA-MB-231, human triple-negative breast cancer cell line; HeLa, human cervical cancer cell line/xenograft; MCF-7, human estrogen receptor–positive breast adenocarcinoma cell line.*

Nanoplatform	Therapy / Imaging	Targeting	Experimental Model	Key Outcome	Ref
GP-GdN@CQDs-MWCNTs/DOX-EGFR (genipin-crosslinked GdN@CQD-decorated MWCNTs, DOX-loaded, anti-EGFR antibody conjugated)	PTT + Chemo (808 nm) / FL + MRI	Active (EGFR antibody)	*In vitro*: A549, MDA-MB-231. *In vivo*: nude mouse xenograft (intratumoral injection, 808 nm irradiation)	Complete tumor elimination, no regrowth at 14 days; pH/NIR-triggered DOX release augments PTT; photothermal conversion efficiency 45.3%; FL confirmed tumor accumulation by confocal imaging of tumor sections; MRI characterized *in vitro* (r1 = 7.178 $mM^{-1}s^{-1}$) and used for liver imaging *in vivo*. No *in vivo* tumor-specific MRI reported.	(8)
rGO/[PEDOT:DPSM]:C/B-PgP (rGO hybridized with ionic PEDOT complex and catechol-BODIPY PEG copolymer)	PTT (808 nm) / FL (pH-responsive, turn-on at acidic pH)	None (passive diffusion)	*In vitro*: KB cells, MDA-MB-231 cells	Temperature ~64°C at 1 mg/mL under 808 nm; <24% cell viability after NIR at 1 mg/mL; pH-responsive fluorescence brightest in acidic conditions, quenched at physiological pH. No *in vivo* data.	(9)
Red-emissive C-dots (PPA-derived carbon dots)	PTT (671 nm) / FL + PA	Passive (EPR)	*In vitro*: HeLa cells*In vivo*: HeLa xenograft, nude mice (IV)	Photothermal conversion efficiency 38.5% at 671 nm; tumor temperature >60°C within 10 min; significant tumor regression in mice; no major organ toxicity observed.	(10)
Au585@AIE-PS nanodots (Au nanostars, LSPR at 585 nm, combined with AIE photosensitizer dots)	PDT (white light, 100 mW/cm^2) / FL (red emission ~665 nm)	None (no targeting ligand reported)	*In vitro*: HeLa cells only	>80% HeLa cell kill in 10 min; 15-fold singlet oxygen generation enhancement vs AIE-PS dots alone; fluorescence enhanced without quenching; low dark cytotoxicity at 10 µg/mL. No *in vivo* data.	(13)
HA-CDs (hyaluronic acid-derived carbon dots)	PDT (650 nm) / FL	Active (CD44 receptor via HA residue)	*In vitro*: A549, 4T1 (CD44-high), L929 (CD44-low) cells	Selective ROS-mediated killing of CD44-high A549 and 4T1 cells under 650 nm irradiation; viability reduced to ~20–30%; L929 (CD44-low) cells largely unaffected; CD44 blocking with free HA confirms receptor-mediated uptake.	(14)

Continued Table 1. *This table summarizes representative preclinical nanoplatforms (material class and formulation features) and links each to its therapy modality (e.g., chemotherapy, photothermal therapy [PTT], photodynamic therapy [PDT], radiotherapy enhancement, immunomodulation), imaging modality (e.g., fluorescence [FL], photoacoustic [PA], MRI, CT, PET), and targeting strategy (passive/enhanced permeability and retention [EPR] vs. active ligand–receptor targeting). Abbreviations: IV, intravenous; SubQ, subcutaneous mouse flank xenograft; U87MG, human glioblastoma xenograft; Raji, human B-cell lymphoma xenograft; KB, human oral epidermoid carcinoma cell line; MDA-MB-231, human triple-negative breast cancer cell line; HeLa, human cervical cancer cell line/xenograft; MCF-7, human estrogen receptor–positive breast adenocarcinoma cell line.*

Nanoplatform	Therapy / Imaging	Targeting	Experimental Model	Key Outcome	Ref
Mn/HA-CDs (single-atom Mn anchored on HA-derived carbon dots via Mn-N5 coordination)	PDT (400–500 nm LED) / FL + MRI (T1-T2 dual-mode)	Mitochondrial self-targeting (Mn uptake by mitochondria)	*In vitro*: HepG2 cells and HepG2 3D multicellular spheroids. *In vivo*: zebrafish embryos (FL imaging and toxicity assessment, 96 hpf)	$^1O_2$ QY = 0.40 (3x vs HA-CDs alone); mitochondrial colocalization coefficient 0.9; inhibits MnSOD, amplifying ROS damage; significant growth inhibition of HepG2 3D spheroids with LED irradiation; T1-T2 dual-mode MRI confirmed *in vitro*; zebrafish showed no significant phenotypic toxicity. No *in vivo* tumor model was reported.	(15)
Se/N-CDs (selenium and nitrogen co-doped carbon dots)	PDT (550 nm LED) / FL + MRI (T2-weighted)	RNA-mediated nuclear localisation	*In vitro*: MCF-7 cells. *In vivo*: 4T1 mouse xenograft (intratumoral injection)	<10% MCF-7 viability at 7.5 μg/mL with light; nuclear envelope penetration enables DNA-proximal ROS generation; significant tumor growth inhibition *in vivo* confirmed by T2-MRI; nuclear membrane disruption confirmed by imaging. Undoped CDs (non-nuclear) showed minimal PDT effect.	(16)
TP-CDs (N-doped red-emissive two-photon carbon dots, PAB-derived)	PDT (638 nm) / Two-photon FL (~605 nm)	RNA-mediated nucleolus targeting	*In vitro*: HeLa cells (PDT efficacy); 4T1 cells (FL imaging only). *In vivo*: biocompatibility only (Balb/c mice); tumor efficacy not assessed	~22% HeLa viability at 100 μg/mL after 638 nm irradiation; real-time FL decrease during PDT reports RNA degradation; no organ toxicity at 14 days *in vivo*. 4T1 was used for fluorescence imaging verification only, not PDT efficacy. *In vivo* antitumor efficacy not tested.	(17)
Cu-CDs (copper-doped carbon dots from Cu-poly(acrylic acid) complex)	PDT / FL	Passive	*In vitro*: HeLa cells (monolayer) + SH-SY5Y 3D multicellular spheroids	$^1O_2$ QY ~36%; FL QY ~24.4%; strong inhibition of HeLa monolayer and SH-SY5Y 3D spheroid growth after light exposure; negligible dark cytotoxicity. No *in vivo* data.	(20)
SWCNT@MS-PEG/DOX (mesoporous silica-coated PEGylated SWCNTs loaded with doxorubicin)	PTT + Chemo (808 nm) / PA + MRI	Passive (EPR)	*In vitro*: 4T1, HeLa, 293T cells*In vivo*: 4T1 breast cancer mouse xenograft (IV, 808 nm)	Tumor temperature ~48°C under 808 nm; PA and MRI confirm tumor accumulation after IV injection; NIR-triggered DOX release; PTT + chemo achieves greater tumor suppression than either monotherapy alone.	(21)

Continued Table 1. *This table summarizes representative preclinical nanoplatforms (material class and formulation features) and links each to its therapy modality (e.g., chemotherapy, photothermal therapy [PTT], photodynamic therapy [PDT], radiotherapy enhancement, immunomodulation), imaging modality (e.g., fluorescence [FL], photoacoustic [PA], MRI, CT, PET), and targeting strategy (passive/enhanced permeability and retention [EPR] vs. active ligand–receptor targeting). Abbreviations: IV, intravenous; SubQ, subcutaneous mouse flank xenograft; U87MG, human glioblastoma xenograft; Raji, human B-cell lymphoma xenograft; KB, human oral epidermoid carcinoma cell line; MDA-MB-231, human triple-negative breast cancer cell line; HeLa, human cervical cancer cell line/xenograft; MCF-7, human estrogen receptor–positive breast adenocarcinoma cell line.*

Nanoplatform	Therapy / Imaging	Targeting	Experimental Model	Key Outcome	Ref
Mn-CD assembly (magnetofluorescent Mn-CDs from Mn-phthalocyanine, co-assembled with DSPE-PEG)	PDT (635 nm) + hypoxia relief (H_2O_2 catalysis) / NIR FL (745 nm) + T1-MRI (r1 = 6.97 $mM^{-1}s^{-1}$)	Passive (EPR via DSPE-PEG coating)	*In vitro*: HeLa cells (simulated tumor microenvironment) *In vivo*: 4T1 tumor-bearing nude mice (IV)	$^1O_2$ QY = 0.40; catalyzes H_2O_2 to O_2, alleviating tumor hypoxia; ~99% HeLa cell death in simulated acidic/H_2O_2 conditions; complete tumor elimination in 4T1 mice with 635 nm light; FL/MRI bimodal imaging guides therapy *in vivo*.	(23)
FA-GdNS@ CQDs-DOX (S, N, Gd tri-doped magnetofluorescent CQDs conjugated with folic acid, loaded with DOX)	Chemo / FL + MRI (dual-modal)	Active (folate receptor via folic acid conjugation)	*In vitro*: HeLa, HepG2, L929 cells*In vivo*: zebrafish (FL imaging only; no mouse tumor efficacy model)	~80% DOX loading efficiency; pH-sensitive release (62% at pH 5.0 vs <12% at pH 7.4 in 3 h); higher MRI signal in HeLa vs HepG2 confirms folate-receptor specificity; enhanced cytotoxicity vs free DOX in HeLa; FL imaging in zebrafish confirms *in vivo* biocompatibility.	(25)

Photothermal Therapy

PTT uses light to induce a therapeutic effect. In PTT, NIR light is absorbed and converted to localized heat that ablates tumor cells (2). Heating can be preferentially localized to nanoparticle-enriched tissue exposed to NIR light, thereby reducing harm to untargeted cells (Figure 1a) (2). PTT is functionally localized because photothermal agents are designed to accumulate in tumors more than in normal tissue via the EPR effect and active targeting, and clinicians restrict where the laser goes via focused beam, image guidance, or fiber delivery. For example, a graphene oxide–polymer hybrid heated from approximately 32°C to approximately 64°C within 5 minutes under 808 nm light and killed about 80% of cancer cells *in vitro* (9). This result was obtained in a KB and MDA-MB-231 cell culture model; comparable studies in *in vivo* tumor environments and in animal models would be needed to further characterize heating profiles and cell-killing efficiency. The same platform also showed pH-responsive fluorescence, which is relevant because the tumor microenvironment is often mildly acidic, and intracellular trafficking after uptake places nanoparticles in acidic endosomes and lysosomes. A pH-activated signal can improve tumor-to-background contrast and help outline tumor margins, supporting image-guided irradiation. Beyond carbon systems, diverse nanostructures support PTT. Reported PTT materials include gold nanorods, graphene-based composites, and carbon-nanotube variants (2, 3). PTT platforms can be constructed to simultaneously visualize and thermally ablate tumor tissue in preclinical models while aiming to spare healthy tissues (2, 10).

Photodynamic Therapy

In contrast to heat-driven ablation, PDT generates cytotoxic ROS upon light activation (Figure 1b) (11, 12). Nanotheranostic designs enhance PDT by coupling photosensitizers with targeting and imaging components so that the diagnostic readout directly informs therapeutic delivery, consistent with the platform definition established in this review (13, 14).

For example, gold-nanostar aggregation-induced

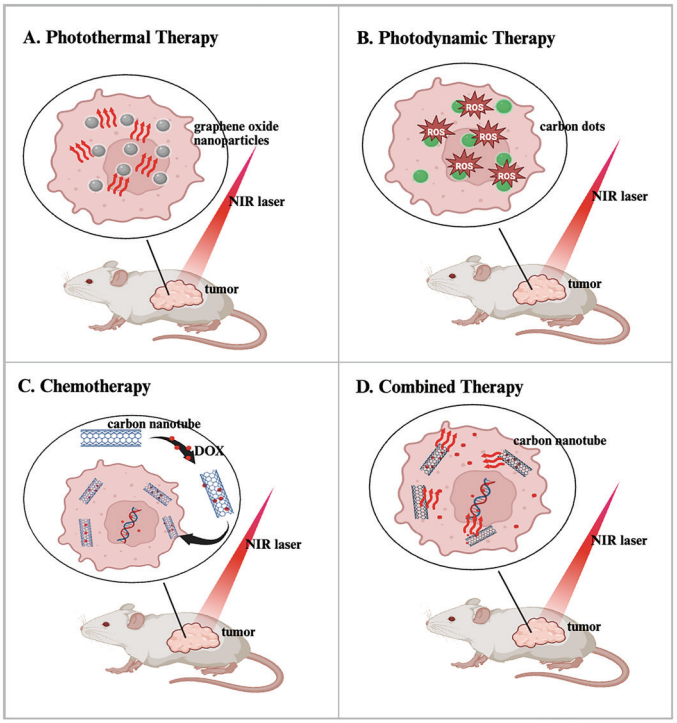

Figure 1. *Nanotheranostic carbon platforms integrate imaging and therapy. (A) PTT: Nanoparticles accumulate in the tumor and, under NIR laser irradiation, generate localized heat for photothermal ablation. (B) PDT: Nanoparticles activated by visible or NIR light generate reactive oxygen species (ROS) inside tumor tissue, causing photodynamic cell death. (C) Carbon nanotubes carrying doxorubicin (DOX) enter tumor cells via endocytosis and release the drug. (D) Carbon nanotubes loaded with DOX release the drug upon irradiation while simultaneously generating heat for combined chemo-photothermal therapy.*

emission (AIE) nanodots provide bright fluorescence for imaging and efficient singlet-oxygen generation (SOG) for PDT. *In vitro*, approximately 80% of cancer cells were killed within 10 minutes of light exposure, versus approximately 18% with the photosensitizer alone (13).

Hyaluronic acid-derived carbon dots (HA-CDs) bind to CD44, a hyaluronic acid receptor frequently overexpressed in many carcinomas and often used as a tumor-associated uptake marker. The HA–CD44 interaction enhances cellular internalization in CD44-high tumors and increases the selectivity of PDT compared to non-targeted uptake (14). Under 650 nm irradiation, HA-CDs generate ROS and selectively reduce viability in CD44-high cells while providing fluorescence for imaging (14). This platform exemplifies ligand-mediated active targeting as a strategy for improving tumor selectivity over EPR-dependent passive accumulation alone, particularly for smaller nanoparticles such as CDs, which are often below the size range most favorable for EPR-driven uptake (14).

Incorporating manganese (Mn) into HA-CDs, specifically by anchoring single-atom Mn on CDs, resulted in mitochondrial colocalization and enhanced ROS-mediated mitochondrial damage (15). This finding is notable because mitochondria play a central role in redox regulation and apoptosis signaling, and ROS generated in close proximity to mitochondria more effectively disrupt mitochondrial membrane potential and drive cell death compared to ROS generated at more distal cellular sites (15). Organelle-proximal ROS delivery may enhance PDT efficacy given the short lifetime and limited diffusion distance of ROS within cells. Reproducible single-atom catalyst loading at scale remains an open manufacturing challenge for this platform class (15).

Selenium/nitrogen (Se/N) co-doped carbon dots were reported to enable nuclear delivery and stronger PDT efficacy through a mechanistically distinct route: producing ROS at or near the nucleus increases the probability of direct DNA damage and replication stress, which can drive rapid loss of viability (16). The authors describe RNA-associated localization and light-triggered nuclear entry to explain why Se/N-doped CDs achieved near-complete *in vitro* cell death after a single light treatment, while undoped CDs, which did not localize to the nucleus, induced minimal cell death (16). In a separate study, two-photon excitable carbon dots reduced HeLa cell viability to approximately 22% under 638 nm irradiation; in mice, intravenous dosing showed no obvious organ toxicity at 14 days. *In vivo* antitumor efficacy has not yet been assessed, representing a necessary step before translational claims can be made (17).

Chemotherapy

Cytotoxic chemotherapy is central to most cancer treatment regimens, yet systemic drug distribution limits both efficacy and tolerability. As illustrated in Figure 1c, nanotheranostic platforms aim to address this by concentrating drugs in tumors and reducing off-target exposure through endocytic uptake and intracellular release (3). One example is polyethylene glycol (PEG)/polyethylenimine (PEI)-functionalized single-walled carbon nanotubes (SWCNTs) loaded with DOX (19). Mechanistically, PEG improves colloidal stability and

prolongs circulation, while PEI increases surface charge and can enhance cellular uptake. Many carriers also use pH-sensitive release because, after uptake, they encounter acidic endosomes and lysosomes, whereas blood and most normal tissues are closer to neutral pH.

Consistent with that design logic, these SWCNTs released >50% of DOX at pH 5.0 by 120 h, versus <40% at pH 7.4 (19). Practically, this points to less premature drug leakage under physiological conditions and more release after cellular internalization. Flow cytometry also showed higher mean fluorescence at 12 h and 24 h compared with free DOX and other carbon nanotube (CNT) carriers (19), which supports higher intracellular drug accumulation. Together, higher uptake plus acid-biased release helps explain why these carriers can increase tumor-cell kill while potentially lowering off-target exposure.

Multi-walled CNTs have also been used as DOX carriers with high loading (~270 mg/g) and faster release at pH 5.0, further accelerated under NIR (8). In mice, combined chemo-photothermal therapy eradicated tumors without regrowth (8). Carbon quantum dot (CQD) polymer nanospheres similarly delivered DOX with pH- and NIR-triggered release (25). By concentrating drugs within tumor cells and timing release to treatment, nanotheranostic carriers have been shown in preclinical models to enhance antitumor effects and may reduce systemic side effects relative to conventional chemotherapy (8, 14, 19).

Combination Platforms

Combination platforms integrate two therapeutic modes (e.g., PTT plus chemotherapy) within one nanoparticle to boost tumor killing while lowering each component's dose (Figure 1d) (13, 16, 20). For example, a PEGylated mesoporous silica-coated SWCNT (SWCNT@MS-PEG) loaded with DOX forms an NIR-responsive system (21): the SWCNT core is the NIR "heater," the silica shell stores the drug, and the PEG coating improves stability and circulation.

Under 808 nm irradiation, local temperatures rise (to ~48 °C in tumors), enabling photothermal damage, enhancing cellular uptake, and promoting intracellular drug release (21). This system was tested on cancer (4T1, HeLa) and non-cancer (293T) cell lines. Combined chemo-photothermal treatment killed more cancer cells than either mode alone, consistent with PTT enhancing drug effectiveness by improving delivery and release.

In representative studies, dual-function designs improve cell killing *in vitro* and, in mice, suppress tumors more effectively than chemotherapy or PTT alone (8, 21). Adding imaging to these carriers makes treatment more controllable. For example, incorporating a T1-weighted MRI contrast component and a fluorescent label into the same carrier can enable confirmation of tumor accumulation before irradiation and support image-guided therapy. Verifying agent location before irradiation allows better timing and localization, reduces off-target effects, and improves reproducibility.

DIAGNOSTICS/IMAGING

Fluorescence imaging offers high sensitivity and cellular-level resolution. Many platforms intrinsically fluoresce or carry fluorescent tags for tumor visualization (10, 20). Copper-doped carbon dots (Cu-CDs) achieved a fluorescence quantum yield of ~24% and a singlet-oxygen yield of ~36%, enabling clear imaging of cancer cells and 3D tumor spheroids while driving PDT to inhibit spheroid growth under light (20). Some nanoparticles extend emission after excitation through afterglow luminescence. The nanoparticles reduce background noise from autofluorescence, providing improved signal-to-noise ratios for imaging tumors.

NIR afterglow AIE dots co-loaded with the AIE fluorophore TPE-Ph-DCM and a Schaap's dioxetane precursor in a lipid-PEG matrix can emit persistently after brief pre-irradiation (22). Reported afterglow lasts >10 days in buffer and has an ~48-min half-life in blood (22). In mice, afterglow imaging yielded ~100× higher tumor-to-liver contrast than conventional fluorescence and enabled image-guided surgery (22). The key advantage is that the signal is collected after excitation is off, which suppresses tissue autofluorescence and boosts tumor-to-background contrast.

Multimodal fluorescent nanoparticles, such as red-emissive CDs, offer both strong fluorescence and photoacoustic signals (ultrasound waves generated when tissue absorbs pulsed light) for dual-mode imaging with photothermal treatment (10). Fluorescent nanotheranostics can also be engineered to respond to tumor-specific triggers such as acidic pH. Solid tumors and intracellular trafficking compartments are often more acidic than blood, so pH-activated ("turn-on") probes can stay dim during circulation and brighten after tumor uptake, improving tumor-to-background contrast. For example, a pH-responsive graphene oxide hybrid remains quenched at physiological pH but fluoresces strongly in acidic conditions typical of tumors, enabling tumor-selective imaging alongside PTT (9). Integrating

imaging with therapy allows real-time monitoring, confirming nanoparticle accumulation, verifying light delivery, and tracking response over time (8, 14, 21, 23).

TARGETING

Targeting is a third component of nanotheranostics: selective tumor accumulation enables potent therapy and high-contrast imaging. The platforms reviewed in this section follow a progression from systemic to cellular to subcellular targeting, moving from passive accumulation through receptor-level binding to organelle-directed delivery (Figure 2).

Passive Targeting

Passive targeting exploits the EPR effect, whereby nanoparticles in the tens-to-hundreds of nanometer size range extravasate through the aberrant, leaky vasculature of tumors and are retained due to impaired lymphatic drainage (Figure 2a). PEGylation extends circulation half-life by reducing opsonization and mononuclear phagocyte system (MPS) clearance, thereby enhancing EPR-mediated tumor accumulation. In a murine xenograft model, PEGylated CNT composites showed increased tumor uptake and elevated apoptosis compared to controls (8). Similarly, SWCNT–PEG–PEI carriers increased cellular uptake and accelerated DOX release at pH 5.0 in MCF-7 breast cancer cells *in vitro* (19). Together, these results support the passive-targeting rationale: prolonged blood residence combined with tumor vascular leakiness increases the probability of nanoparticle accumulation, and acidic intracellular compartments promote drug release following uptake.

Active Targeting

Active targeting uses surface ligands such as antibodies, peptides, and small molecules that bind tumor-associated receptors, promoting receptor-mediated endocytosis and payload internalization. As shown in Figure 2b, hyaluronic acid on the nanoparticle surface binds CD44 receptors overexpressed on tumor cells, driving selective uptake compared to passive accumulation alone. Under 650 nm light, HA-CDs bind CD44 and reduce cancer cell viability to approximately 20–30% while sparing normal cells *in vitro* (14). In a separate study using epidermal growth factor receptor (EGFR)-functionalized multi-walled CNTs, antibody conjugation further improved tumor-cell uptake and increased targeted cytotoxicity compared with non-functionalized carriers (8), suggesting that receptor-specific ligand decoration is a broadly applicable strategy for enhancing active targeting selectivity. In another active-targeting approach, hyaluronic acid caps mesoporous silica nanoparticles, improving tumor-

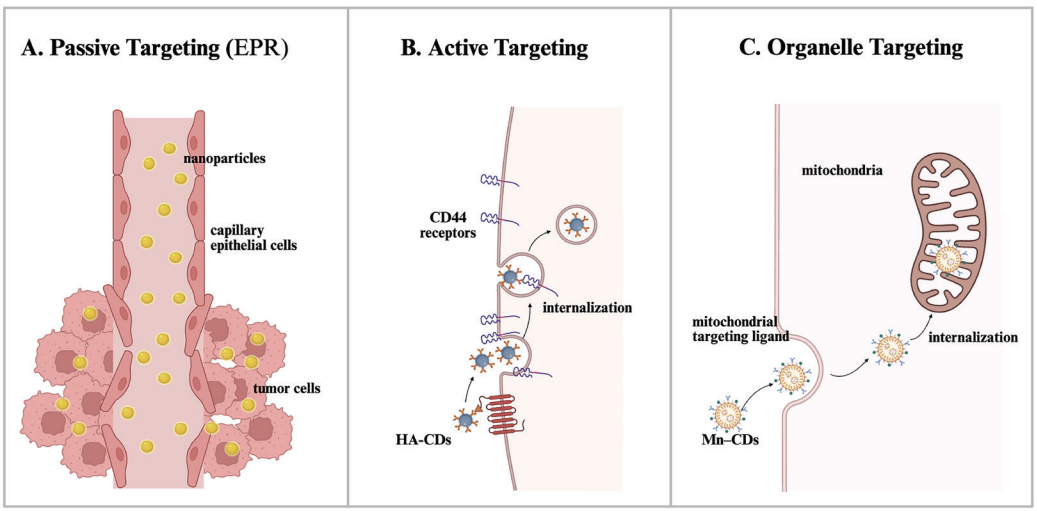

Figure 2. *(a) Nanoparticles circulate in blood and passively accumulate in tumors because tumor vasculature is irregular and leaky (EPR effect), and particles are retained due to poor lymphatic drainage. (b) Surface ligands (e.g., hyaluronic acid) bind receptors such as CD44 on tumor cells, promoting receptor-mediated endocytosis and payload release. (c) Nanoparticles tagged with mitochondrial-targeting ligands enter tumor cells and concentrate in mitochondria, releasing payloads directly within the organelle.*

cell interactions via HA recognition while enabling bioresponsive uncapping and drug release in the tumor microenvironment (24). Folate-mediated active targeting is a well-studied approach because folate receptor-α is overexpressed in several tumor types and can promote receptor-mediated endocytosis when nanoparticles are decorated with folic acid. Folate-functionalized carbon quantum dots have been reported to increase uptake in folate-receptor-positive cells and improve DOX delivery, including pH-responsive release, relative to free drug (25).

Organelle targeting

Nanoparticles can also be functionalized with organelle-targeting ligands to increase efficacy by placing the payload near vulnerable intracellular structures (e.g., mitochondria or the nucleus) (Figure 2c). Organelle targeting can also increase efficacy by placing ROS generation near vulnerable intracellular structures. For example, single-atom Mn anchored on carbon dots increased mitochondrial colocalization and enhanced ROS-mediated mitochondrial damage (15). Nuclear-proximal ROS generation has also been used to intensify PDT by placing oxidative stress closer to DNA (16).

Combining passive accumulation with molecular and organelle-level targeting has been shown in preclinical models to increase tumor specificity. Enhanced targeting concentrates payloads in cancer cells and specific organelles, improves imaging contrast, and may support more effective treatment paradigms in controlled experimental settings (3, 11, 14).

Overall, passive targeting increases the odds of tumor accumulation through pharmacokinetics, active targeting increases cellular uptake through receptor binding, and organelle targeting increases potency by placing the payload where it can do the most damage with minimal diffusion loss.

While the sections above describe therapeutic modalities, diagnostic readouts, and targeting strategies at a mechanistic level, translational readiness depends on additional constraints that cut across all three domains. The following subsection summarizes the most common clinical translation barriers and frames them as design implications for nanotheranostic platforms.

CLINICAL TRANSLATION CONSTRAINTS

The platforms reviewed above demonstrate meaningful preclinical activity, but several constraints limit their path to clinical use.

Immune clearance is a primary obstacle. Nanoparticles that are not adequately surface-shielded are opsonized and removed before reaching tumor sites. PEGylation, used across most platforms reviewed here, extends circulation but can trigger anti-PEG antibody responses with repeated dosing, which may reduce accumulation over a treatment course (2, 6). Even when nanoparticles reach the tumor, batch-to-batch variability introduces a separate concern. For complex platforms such as single-atom Mn-loaded CDs and SWCNT-mesoporous silica composites, size distribution, drug loading, and photosensitizer incorporation can shift across synthesis runs. Without standardized manufacturing controls, the reproducibility required for clinical trials cannot be assured (2, 6).

Beyond consistency in production, the safety profile of these platforms over time remains poorly characterized. The *in vivo* assessments in the reviewed studies are typically limited to 14 days in mice, which is insufficient to determine whether nanoparticle components accumulate in organs over longer timeframes or generate chronic toxicity (2, 17). Finally, even platforms that clear these scientific and manufacturing hurdles face a regulatory challenge. A construct that combines a cytotoxic drug, an imaging agent, and a targeting ligand within a single particle may require review under multiple regulatory frameworks, creating an uncertain approval pathway that differs by jurisdiction (6).

Overall, platforms most likely to translate are those that simplify design, use biodegradable materials, demonstrate reproducible manufacturing, and align with existing clinical imaging and treatment workflows.

CONCLUSION

This review examined nanotheranostic platforms across four therapy modalities (PTT, PDT, chemotherapy, and combination approaches), two primary diagnostic readouts (fluorescence and MRI), and three targeting strategies (passive EPR accumulation, ligand-mediated active targeting, and organelle localization). Several design principles emerge from this body of evidence and are worth making explicit.

On the therapeutic side, combination platforms frequently demonstrated stronger tumor suppression than single-modality comparators within the same experimental system. Combined chemo-photothermal platforms achieved tumor regression at doses where neither DOX alone nor NIR irradiation alone was sufficient (8, 21). This pattern holds because PTT

enhances cellular membrane permeability and promotes intracellular drug release, giving the combination a mechanistic basis rather than simply an additive effect. Platforms that integrate two modes without this mechanistic rationale do not satisfy the same design standard.

On the imaging side, the diagnostic readout must be functionally linked to therapeutic delivery, not merely co-loaded in the same particle. The clearest preclinical results came from platforms where imaging directly guided treatment. In one case, pH-responsive fluorescence confirmed acidic tumor uptake before irradiation (9). In another, afterglow emission enabled real-time surgical guidance by suppressing tissue autofluorescence and raising tumor-to-background contrast to approximately 100-fold over conventional fluorescence (22). Constructs that carry a fluorescent label without using it to inform or verify therapeutic action do not meet the platform definition used throughout this review.

On the targeting side, passive EPR-dependent accumulation is a useful starting point but is insufficient on its own, particularly for smaller particles such as carbon dots that fall below the size range most favorable for EPR-driven uptake (14). Layering active receptor targeting onto a passively accumulating scaffold consistently improved tumor selectivity *in vitro*, as seen with HA-CD44 binding (14, 24). Organelle-level targeting extended this further: mitochondrial-proximal ROS generation and nuclear-proximal oxidative stress both produced stronger cell kill than platforms that generated ROS at non-specific intracellular sites (15, 16). The platforms with the strongest preclinical profiles in this review operated at more than one of these levels simultaneously.

Translational potential depends on how well a platform addresses the barriers outlined in the Clinical Translation section. Platforms built on components with established clinical biocompatibility profiles are better positioned than those relying on novel dopants or catalysts whose long-term clearance remains uncharacterized (2, 6). Complex formulations face unresolved batch-to-batch variability in size distribution, drug loading, and photosensitizer incorporation, which undermines the reproducibility required for clinical trials (2, 6). Regulatory viability also favors platforms in which the therapeutic and diagnostic functions can be independently characterized, enabling a more tractable approval pathway (6).

Multimodal, targeted nanotheranostics that satisfy these criteria may improve outcomes by enabling earlier detection, precise delivery, and real-time response monitoring. Directing research toward these translational constraints, rather than toward continued addition of functional layers, offers a pragmatic path toward platforms that may move from preclinical promise toward more adaptive cancer therapy strategies (2, 3).

ACKNOWLEDGEMENTS

This project was completed under the guidance of a PhD student mentor, Henry Squire.

FUNDING SOURCES

The author did not receive any funding for this research.

CONFLICT OF INTEREST

The author declares no conflicts of interest related to this work.

REFERENCES

1. Bray F, Laversanne M, Sung H, Ferlay J, *et al*. Global cancer statistics 2022: GLOBOCAN estimates of incidence and mortality worldwide for 36 cancers in 185 countries. *CA: A Cancer Journal for Clinicians*. 2024; 74 (3): 229-263. Accessed June 27, 2024. https://pubmed.ncbi.nlm.nih.gov/38572751/. https://doi.org/10.3322/caac.21834
2. Gai S, Yang G, Yang P, He F, *et al*. Recent advances in functional nanomaterials for light-triggered cancer therapy. *Nano Today.* 2018; 19: 146-187. https://doi.org/10.1016/j.nantod.2018.02.010
3. Dai L, Qu Y, Yang S. Carbon nanomaterials for biological imaging and nanomedicinal therapy. *Chem Soc Rev.* 2015; 44 (14): 6023-6057.
4. Welsher K, Sherlock SP, Dai HJ. Deep-tissue anatomical imaging of mice using carbon nanotube fluorophores in the second near-infrared window. *Proc Natl Acad Sci U S A.* 2011; 108: 8943-8948. https://doi.org/10.1073/pnas.1014501108
5. De La Zerda A, Zavaleta C, Keren S, Vaithilingam S, *et al*. Carbon nanotubes as photoacoustic molecular imaging agents in living mice. *Nat Nanotechnol*. 2008; 3: 557-562. https://doi.org/10.1038/nnano.2008.231
6. Chen Z, Wang Z, Gu Z. Bioinspired and biomimetic nanomedicines. *Acc Chem Res.* 2019; 52 (5): 1255-1264. https://doi.org/10.1021/acs.accounts.9b00079
7. Liu Z, Fan AC, Rakhra K, Sherlock S, *et al*.

Supramolecular stacking of doxorubicin on carbon nanotubes for *in vivo* cancer therapy. *Angew Chem Int Ed*. 2009; 48: 7668-7672. https://doi.org/10.1002/anie.200902612

8. Zhang M, Wang W, Wu F, Yuan P, *et al*. Magnetic and fluorescent carbon nanotubes for dual-modal imaging and photothermal and chemo-therapy of cancer cells in living mice. *Carbon*. 2017; 123: 70-83. https://doi.org/10.1016/j.carbon.2017.07.032
9. Sharker SM, Kang EB, Shin C-I, *et al*. NIR-active, pH-responsive rGO hybrid for imaging-guided PTT. *J Appl Polym Sci*. 2016; 133: 43791. https://doi.org/10.1002/app.43791
10. Ge J, Jia Q, Liu W, Guo L, *et al*. Red-emissive carbon dots for fluorescent, photoacoustic, and thermal theranostics in living mice. *Adv Mater.* 2015; 27: 4169-4177. https://doi.org/10.1002/adma.201500323
11. Fan W, Huang P, Chen X. Overcoming the Achilles' heel of photodynamic therapy. *Chem Soc Rev.* 2016; 45: 6488-6519. https://doi.org/10.1039/C6CS00616G
12. Agostinis P, *et al*. Photodynamic therapy of cancer: An update. *CA Cancer J Clin*. 2011; 61 (4): 250-281. https://doi.org/10.3322/caac.20114
13. Yaraki MT, Wu M, Middha E, *et al*. Gold nanostars-AIE theranostic nanodots for image-guided PDT. *Nano-Micro Lett.* 2021; 13: 58. https://doi.org/10.1007/s40820-020-00583-2
14. Zhang L, Lin Z, Yu Y-X, Jiang B-P, Shen X-C. Hyaluronic-acid-derived carbon dots for self-targeted imaging-guided PDT. *J Mater Chem B*. 2018; 6: 6534-6543. https://doi.org/10.1039/C8TB01957F
15. Wang S, Ma M, Liang Q, Wu X, *et al*. Single-atom manganese anchored on carbon dots for promoting mitochondrial targeting and photodynamic effect in cancer treatment. *ACS Appl Nano Mater.* 2022; 5: 6679-6690. https://doi.org/10.1021/acsanm.2c00716
16. Xu N, Du J, Yao Q, *et al*. Se/N-doped carbon dots for precise PDT via nuclear envelope penetration. *Carbon*. 2020; 159: 74-82. https://doi.org/10.1016/j.carbon.2019.12.002
17. Yi S, Deng S, Guo X, *et al*. Red-emissive two-photon CDs for nucleolus-targeted PDT with real-time monitoring. *Carbon*. 2021; 182: 155-166. https://doi.org/10.1016/j.carbon.2021.05.055
18. Biel MA. Photodynamic therapy treatment of early oral and laryngeal cancers. *Photochem Photobiol*. 2007; 83 (5): 1063-1068. https://doi.org/10.1111/j.1751-1097.2007.00153.x
19. Yang S, Wang Z, Ping Y, *et al*. PEG/PEI-functionalized SWCNTs as DOX carriers: Loading/release/uptake. *Beilstein J Nanotechnol*. 2020; 11: 1728-1741. https://doi.org/10.3762/bjnano.11.155
20. Wang J, Xu M, Wang D, *et al*. Copper-doped carbon dots for optical bioimaging and photodynamic therapy. *Inorg Chem*. 2019; 58: 13394-13402. https://doi.org/10.1021/acs.inorgchem.9b02283
21. Liu J, Wang C, Wang X, *et al*. Mesoporous silica-coated SWCNTs for imaging-guided combination therapy. *Adv Funct Mater.* 2015; 25: 384-392. https://doi.org/10.1002/adfm.201403079
22. Ni X, Zhang X, Duan X, *et al*. NIR afterglow AIE dots with ultrahigh tumor-to-liver ratio for image-guided surgery. *Nano Lett*. 2019; 19: 318-330. https://doi.org/10.1021/acs.nanolett.8b03936
23. Jia Q, Ge J, Liu W, Zheng X, *et al*. A magneto-fluorescent carbon dot assembly as an acidic H2O2-driven oxygenator to regulate tumor hypoxia for simultaneous bimodal imaging and enhanced photodynamic therapy. *Adv Mater*. 2018; 30: 1706090. https://doi.org/10.1002/adma.201870093
24. Chen Z, Li Z, Lin Y, Yin M, *et al*. Bioresponsive hyaluronic acid-capped mesoporous silica nanoparticles for targeted drug delivery. *Chem Eur J*. 2013; 19: 1778-1783. https://doi.org/10.1002/chem.201202038
25. Chiu SH, Gedda G, Girma WM, Chen JK, *et al*. Rapid fabrication of carbon quantum dots as multifunctional nanovehicles for dual-modal targeted imaging and chemotherapy. *Acta Biomater.* 2016; 46: 151-164. https://doi.org/10.1016/j.actbio.2016.09.027